Available online at www.sciencedirect.com
SCIENCE DIRECT®
Journal of Solid State Chemistry 178 (2005) 1722–1737
JOURNAL OF SOLID STATE CHEMISTRY
www.elsevier.com/locate/jssc

Synthesis, characterization and thermal properties of small $R_2R'_2N^+X^-$-type quaternary ammonium halides

Sara Busi[a], Manu Lahtinen[a,*], Heidi Mansikkamäki[b], Jussi Valkonen[a], Kari Rissanen[b]

[a]Department of Chemistry, University of Jyväskylä, P.O. Box 35, FIN-40014 Jyväskylän yliopisto, Finland
[b]NanoScience Center, Department of Chemistry, University of Jyväskylä, P.O. Box 35, FIN-40014 Jyväskylän yliopisto, Finland

Received 22 December 2004; received in revised form 22 December 2004
Available online 21 April 2005

Abstract

Twenty-one $R_2R'_2N^+X^-$ -type (R = methyl or ethyl, R' = alkyl, X = Br or I) quaternary ammonium (QA) halides have been prepared by using a novel one-pot synthetic route in which a formamide (dimethyl-, diethylformamide, etc.) is treated with alkyl halide in the presence of sodium or potassium carbonate. The formation of QA halides was verified with ^{1}H-NMR, ^{13}C-NMR, MS and elemental analysis. The crystal structures of four QA halides (two bromide and two iodide) were determined using X-ray single crystal diffraction, and the powder diffraction method was used to study the structural similarities between the single crystal and microcrystalline bulk material. The thermal properties of all compounds were studied using TG/DTA and DSC methods. The smallest compounds decomposed during or before melting. The decreasing trend of melting points was observed when the alkyl chain length was increased. The liquid ranges of 120–180 °C were observed for compounds with 5–6 carbon atoms in the alkyl chain. The low melting points and wide liquid ranges suggest potential applicability of these compounds for example as ionic liquids precursors.

Keywords: Quaternary ammonium bromide; Quaternary ammonium iodide; Ionic liquid; X-ray single crystal diffraction; X-ray powder diffraction; Thermal analysis

1. Introduction

The quaternary ammonium (QA) halides have been synthesized and studied for a long time [1–12], those studies being mainly concentrated on their properties as surfactants [12–16] and catalysts [17,18]. The alkyl substituted QA bromides have also been used significantly as electrolytes for example in Zn/Br batteries [19–22]. The smallest QA halides have shown to be useful quest candidates for resorcinarene complexation, as the QA cations have the possibility to interact via cation–π and C–H–π interactions as well as fill the hollow cavity of the electron rich resorcinarene host [23–27].

Thermodynamic properties as well as viscosity, solubility, density, mobility and conductivity measurements of several QA compounds in various solution conditions are widely reported [28–38]. Also, some studies having NMR and MS measurements are known [39–42]. However, the basic characterization, X-ray single crystal analysis and thermal properties of these small QA compounds, especially $R_2R'_2N^+X^-$-type QA compounds, have drawn less attention. In this study, we describe the syntheses and characterizations of 21 small $R_2R'_2N^+X^-$-type QA halides (12 bromides and 9 iodides). Five of them have already been introduced shortly in our previous publication [43] in which the novel one-pot synthesis route of QA halides was described. ^{1}H-NMR and ^{13}C-NMR spectroscopy, ESI-TOF MS measurements and elemental analysis were used for the characterisation of the presented

*Corresponding author. Fax: +358 14 260 2501.
E-mail address: makrla@cc.jyu.fi (M. Lahtinen).

0022-4596/$ - see front matter © 2005 Elsevier Inc. All rights reserved.
doi:10.1016/j.jssc.2005.03.008

compounds. Furthermore, the X-ray single crystal structures of four compounds were solved and are described in details. The powder diffraction data were measured to investigate the crystalline content of the compounds, and also to confirm the structural similarities between the single crystal structures and microcrystalline bulk material. The thermal behaviour of the compounds was determined with TG/DTA and DSC methods. The aim of this study, as well as the previous studies [43,44], is to develop new type of QA halides and eventually by changing the anion type of these halides to alter their physical and chemical properties more suitable for ionic liquid applications [45–48], in which for example a low melting point, thermal stability, density, viscosity and solubility are key issues.

Ionic liquids represent a new kind of class of solvents, which are liquid at low temperature (typically below 100 °C) and have relatively low viscosity [45]. QA compounds have proven one potential group for ionic liquids. As early as 1914, ethylammonium nitrate was found liquid at room temperature though it contained small amounts of water [49]. Swain et al. used tetra-*n*-hexylammonium benzoate as a solvent for kinetic and electrochemical investigations already at 1967 [50]. Wasserchеid et al. have reviewed the synthesis, properties, and potential of ionic liquids with respect to their application as solvent in transition metal catalysis [45]. Recently, ionic liquids have attracted worldwide interest showing their potential over conventional organic solvents in certain reaction processes and/or as a catalyst in transition metal and in Friedel–Craft catalyst and in various polymer processes [51–69]. Generally, ionic liquids can be synthesized for example by quaternization of an amine or phosphane to form the cation. The imidazolium ion, pyridium ion, ammonium ion and phosphonium ion have found important types of cation in ionic liquids and by changing the cation/anion combinations the numerous ionic liquids with melting points below 100 °C can be achieved [45].

2. Experimental section

2.1. Synthesis

General procedure: The compounds **1–21** (Scheme 1) were synthesized by using a one-pot synthetic route in

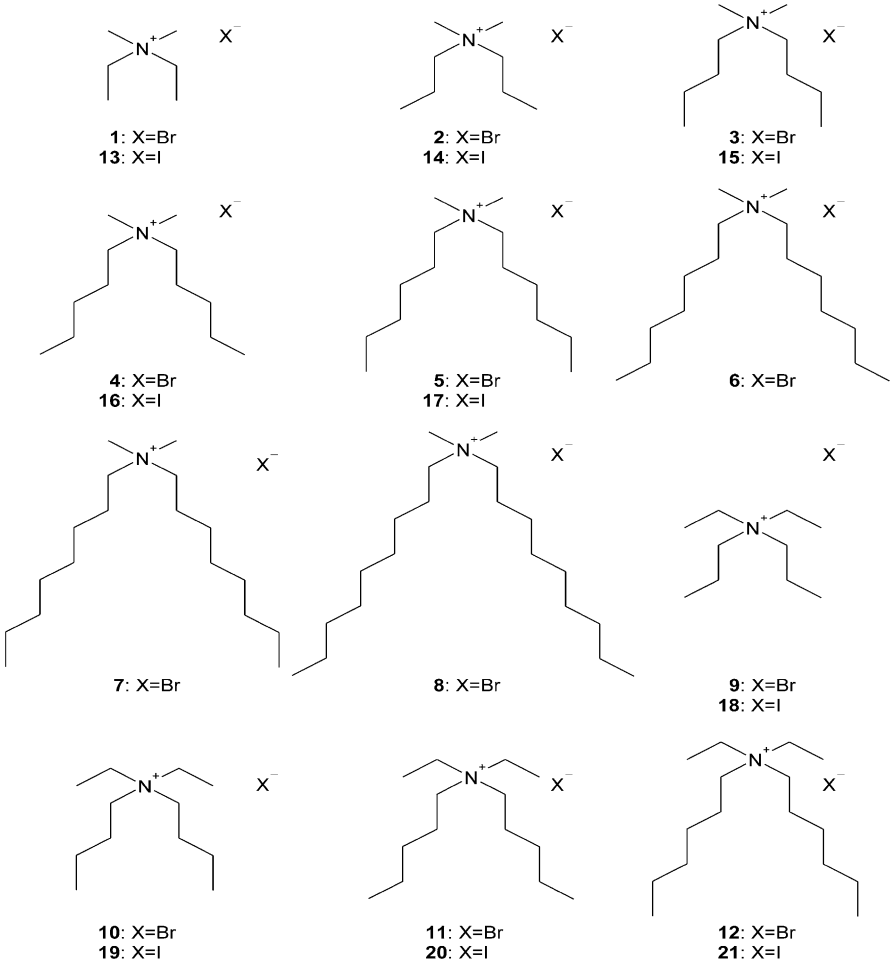

Scheme 1. Molecular structures of the compounds **1–21**.

which a formamide is treated with alkyl halide in the presence of potassium or sodium carbonate [43]. All reactants and other chemicals are commercially available and were used as received.

All the reagents were placed in the reaction flask. The reaction mixture was stirred at chosen temperature for 48–72 h. After cooling down to RT the mixture was filtered and the filtrate was evaporated. The extraction of the product was performed with one of the following methods.

Method A: A small amount of acetone, diethyl ether, toluene or mixture of these was added to the residue to give a white or light brown powder. The powder was washed with diethyl ether and dried in vacuo over night.

Method B: Evaporation of filtrate gave the product as a pure gel. The gel was dried in vacuo.

Method C: As method B but after drying in vacuo the product was precipitated from gel by adding diethyl ether to the residue. The powder was dried in vacuo over night.

Method D: The residue (from evaporation of filtrate) was dissolved to water/diethyl ether solution. The water layer was separated and evaporated giving the product as a pure gel. The gel was dried in vacuo.

Method E: Evaporation of filtrate gave the raw product as a white or yellow powder. The product was extracted by dissolving it to dichloromethane and the final product was obtained by evaporation of the filtrate. The powder was dried in vacuo over night.

Diethyldimethylammonium bromide **(1)**: Method A. Reagents: ethyl bromide (6.51 ml, 87.86 mmol), potassium carbonate (18.21 g, 131.80 mmol) and dimethyl formamide (50 ml). Reaction temperature 35 °C and reaction time 66 h. Yield (white sticky powder): 1.92 g (24%). ^{1}H-NMR ($CDCl_3$, 500 MHz, ppm): 1.29 (6H, t, $J = 7.29$ Hz, N-$CH_2C\mathbf{H}_3$), 3.20 (6H, s, N-$C\mathbf{H}_3$), 3.56 (4 H, q, $J = 7.30$ Hz, N-$C\mathbf{H}_2CH_3$). ^{13}C NMR ($CDCl_3$, 126 MHz, ppm): 8.26 (2C, N-$CH_2\mathbf{C}H_3$), 49.81 (2C, N-$\mathbf{C}H_3$), 58.78 (2C, N-$\mathbf{C}H_2CH_3$). ESI-TOF-MS: m/z calculated for $C_6H_{16}NBr$ $[M\text{-}Br]^+$: 102.13; found: 102.08 $[M\text{-}Br]^+$. Elemental analysis: Calculated for $C_6H_{16}NBr$: C, 39.57; H, 8.86; N, 7.69. Found: C, 41.00; H, 8.81; N, 6.27. (Very hygroscopic and sticky even after drying; results match when water and crystallization solvent, toluene, is added.)

Dimethyldipropylammonium bromide **(2)**: Method A. Reagents: propyl bromide (8.64 ml, 95.17 mmol), potassium carbonate (9.86 g, 71.38 mmol) and dimethyl formamide (30 ml). Reaction temperature 65 °C and reaction time 72 h. Yield (white powder) 3.11 g (31%). ^{1}H-NMR ($CDCl_3$, 500 MHz, ppm): 1.03 (6H, t, $J = 7.32$ Hz, N-$CH_2CH_2C\mathbf{H}_3$), 1.78 (4H, m, N-$CH_2C\mathbf{H}_2CH_3$), 3.39 (6H, s, N-$C\mathbf{H}_3$), 3.51 (4H, m, N-$C\mathbf{H}_2CH_2CH_3$). ^{13}C NMR ($CDCl_3$, 126 MHz, ppm): 10.64 (2C, N-$CH_2CH_2\mathbf{C}H_3$), 16.29 (2C, N-$CH_2\mathbf{C}H_2CH_3$), 51.22 (2C, N-$\mathbf{C}H_3$), 65.48 (2C, N-$\mathbf{C}H_2CH_2CH_3$). ESI-TOF-MS: m/z calculated for $C_8H_{20}NBr$ $[M\text{-}Br]^+$: 130.16; found: 130.12 $[M\text{-}Br]^+$. Elemental analysis: Calculated for $C_8H_{20}NBr$: C, 45.72; H, 9.59; N, 6.66. Found: C, 45.06; H, 9.72; N, 6.69.

Dibutyldimethylammonium bromide **(3)**: Method A. Reagents: butyl bromide (9.02 ml, 83.96 mmol), potassium carbonate (8.70 g, 62.97 mmol) and dimethyl formamide (30 ml). Reaction temperature 80 °C and reaction time 72 h. Yield (white powder) 2.42 g (24%). ^{1}H-NMR ($CDCl_3$, 500 MHz, ppm): 0.95 (6 H, t, $J = 7.36$ Hz, N-$CH_2CH_2CH_2C\mathbf{H}_3$), 1.41 (4 H, sextet, $J = 7.42$ Hz, N-$CH_2CH_2C\mathbf{H}_2CH_3$), 1.67 (4H, m, N-$CH_2C\mathbf{H}_2CH_2CH_3$), 3.35 (6H, s, N-$C\mathbf{H}_3$), 3.53 (4H, m, N-$C\mathbf{H}_2CH_2CH_2CH_3$). ^{13}C NMR ($CDCl_3$, 126 MHz, ppm): 13.59 (2C, N-$CH_2CH_2CH_2\mathbf{C}H_3$), 19.51 (2C, N-$CH_2CH_2\mathbf{C}H_2CH_3$), 24.57 (2C, N-$CH_2\mathbf{C}H_2CH_2CH_3$), 51.10 (2C, N-$\mathbf{C}H_3$), 63.74 (2C, N-$\mathbf{C}H_2CH_2CH_2CH_3$). ESI-TOF-MS: m/z calculated for $C_{10}H_{24}NBr$ $[M\text{-}Br]^+$: 158.19; found: 158.15 $[M\text{-}Br]^+$. Elemental analysis: Calculated for $C_{10}H_{24}NBr$: C, 50.42; H, 10.16; N, 5.88. Found: C, 50.72; H, 10.43; N, 5.95.

Dimethyldipentylammonium bromide **(4)**: Method B. Reagents: pentyl bromide (9.32 ml, 75.12 mmol), potassium carbonate (10.38 g, 75.12 mmol) and dimethyl formamide (30 ml). Reaction temperature 80 °C and reaction time 69 h. Yield (brown partially microcrystalline gel) 3.19 g (32%). ^{1}H-NMR ($CDCl_3$, 500 MHz, ppm): 0.88 (6H, t, $J = 6.88$ Hz, N-$CH_2CH_2CH_2CH_2C\mathbf{H}_3$), 1.35 (8H, m, N-$CH_2CH_2(C\mathbf{H}_2)_2CH_3$), 1.68 (4H, m, N-$CH_2C\mathbf{H}_2CH_2CH_2CH_3$), 3.37 (6H, s, N-$C\mathbf{H}_3$), 3.51 (4H, m, N-$C\mathbf{H}_2$-). ^{13}C NMR ($CDCl_3$, 126 MHz, ppm): 13.92 (2C, N-$CH_2CH_2CH_2CH_2\mathbf{C}H_3$), 22.40 and 22.61 (4C, N-$CH_2CH_2(\mathbf{C}H_2)_2CH_3$), 28.40 (2C, N-$CH_2\mathbf{C}H_2$-), 51.36 (2C, N-$\mathbf{C}H_3$), 64.09 (2C, N-$\mathbf{C}H_2$-). ESI-TOF-MS: m/z calculated for $C_{12}H_{28}NBr$ $[M\text{-}Br]^+$: 186.22; found: 186.19 $[M\text{-}Br]^+$. Elemental analysis: Calculated for $C_{12}H_{28}NBr$: C, 54.13; H, 10.60; N, 5.26. Found: C, 53.85; H, 10.56; N, 5.21.

Dihexyldimethylammonium bromide **(5)**: Method D. Reagents: hexyl bromide (13.09 ml, 93.28 mmol), potassium carbonate (9.67 g, 69.96 mmol) and dimethyl formamide (30 ml). Reaction temperature 80 °C and reaction time 70 h. Yield (yellow partially microcrystalline gel) 2.81 g (28%). ^{1}H-NMR ($CDCl_3$, 500 MHz, ppm): 0.79 (6H, t, $J = 7.10$ Hz, N-$CH_2CH_2CH_2CH_2CH_2C\mathbf{H}_3$), 1.20–1.31 (12H, m, N-$CH_2CH_2(C\mathbf{H}_2)_3CH_3$), 1.61 (4H, m, N-$CH_2C\mathbf{H}_2$-), 3.30 (6H, s, N-$C\mathbf{H}_3$), 3.45 (4H, m, N-$C\mathbf{H}_2$-). ^{13}C NMR ($CDCl_3$, 126 MHz, ppm): 13.62 (2C, N-$CH_2CH_2CH_2CH_2CH_2\mathbf{C}H_3$), 22.51 (2C, N-$CH_2\mathbf{C}H_2$-), 22.13, 25.66 and 31.03 (6C, N-$CH_2CH_2(\mathbf{C}H_2)_3CH_3$), 50.99 (2C, N-$\mathbf{C}H_3$), 63.78 (2C, N-$\mathbf{C}H_2$-). ESI-TOF-MS: m/z calculated for $C_{14}H_{32}NBr$ $[M\text{-}Br]^+$: 214.25; found: 214.29 $[M\text{-}Br]^+$. Elemental analysis: Calculated for $C_{14}H_{32}NBr$: C, 57.13; H, 10.96; N, 4.76. Found: C, 56.83; H, 11.05; N, 4.69.

Diheptyldimethylammonium bromide **(6)**: Method D. Reagents: heptyl bromide (12.96 ml, 82.49 mmol), potassium carbonate (8.55 g, 61.87 mmol) and dimethyl formamide (30 ml). Reaction temperature 80 °C and reaction time 48 h. Yield (yellow gel) 1.89 g (19%). ^{1}H-NMR ($CDCl_3$, 500 MHz, ppm): 0.66 (6H, t, J = 6.88 Hz, N-$CH_2CH_2CH_2CH_2CH_2CH_2CH_3$), 1.05–1.20 (16H, m, N-$CH_2CH_2(CH_2)_4CH_3$), 1.51 (4H, m, N-$CH_2CH_2$-), 3.16 (6H, s, N-$CH_3$), 3.34 (4H, m, N-$CH_2$-). ^{13}C NMR ($CDCl_3$, 126 MHz, ppm): 13.45 (2C, N-$CH_2CH_2CH_2CH_2CH_2CH_2CH_3$), 22.26 (2C, N-$CH_2CH_2$-), 21.89, 25.66, 28.28 and 30.96 (8C, N-$CH_2CH_2(CH_2)_4CH_3$), 50.67 (2C, N-CH_3), 63.53 (2C, N-CH_2-). ESI-TOF-MS: m/z calculated for $C_{16}H_{36}NBr$ $[M\text{-}Br]^+$: 242.28; found: 242.32 $[M\text{-}Br]^+$. Elemental analysis: Calculated for $C_{16}H_{36}NBr$: C, 59.61; H, 11.26; N, 4.34. Found: C, 58.80; H, 11.32; N, 4.20.

Dimethyldioctylammonium bromide **(7)**: Method C. Reagents: octyl bromide (7.43 ml, 42.80 mmol), potassium carbonate (5.91 g, 42.80 mmol) and dimethyl formamide (50 ml). Reaction temperature 85 °C and reaction time 68 h. Yield (yellowish microcrystalline gel) 0.70 g (17%). ^{1}H-NMR ($CDCl_3$, 500 MHz, ppm): 0.79 (6H, t, J = 5.77 Hz, N-$CH_2CH_2(CH_2)_5CH_3$), 1.18–1.30 (20H, m, N-$CH_2CH_2(CH_2)_5CH_3$), 1.63 (4H, m, N-CH_2CH_2-), 3.32 (6H, s, N-CH_3), 3.46 (4H, m, N-CH_2-). ^{13}C NMR ($CDCl_3$, 126 MHz, ppm): 13.80 (2C, N-$CH_2CH_2(CH_2)_5CH_3$), 22.59 (2C, N-CH_2CH_2-), 22.32, 26.04, 28.79, 28.93 and 31.40 (10C, N-$CH_2CH_2(CH_2)_5CH_3$), 51.05 (2C, N-CH_3), 63.72 (2C, N-CH_2-). ESI-TOF-MS: m/z calculated for $C_{18}H_{40}NBr$ $[M\text{-}Br]^+$: 270.32; found: 270.36 $[M\text{-}Br]^+$. Elemental analysis: Calculated for $C_{18}H_{40}NBr$: C, 61.70; H, 11.51; N, 4.00. Found: C, 60.85; H, 11.56; N, 3.84.

Dimethyldinonylammonium bromide **(8)**: Method D. Reagents: nonyl bromide (10.10 ml, 52.84 mmol), potassium carbonate (5.48 g, 39.63 mmol) and dimethyl formamide (30 ml). Reaction temperature 80 °C and reaction time 50 h. The gel solidified partly during drying in vacuo. Yield (yellowish microcrystalline gel) 1.45 g (15%). ^{1}H-NMR ($CDCl_3$, 500 MHz, ppm): 0.81 (6H, t, J = 6.71 Hz, N-$CH_2CH_2(CH_2)_6CH_3$), 1.19–1.31 (26H, m, N-$CH_2CH_2(CH_2)_6CH_3$), 1.64 (4H, m, N-CH_2CH_2-), 3.34 (6H, s, N-CH_3), 3.47 (4H, m, N-CH_2-). ^{13}C NMR ($CDCl_3$, 126 MHz, ppm): 13.86 (2C, N-$CH_2CH_2(CH_2)_6CH_3$), 22.63 (2C, N-CH_2CH_2-), 22.41, 26.08, 28.91, 29.02, 29.13 and 31.57 (12C, N-$CH_2CH_2(CH_2)_6CH_3$), 51.10 (2C, N-CH_3), 63.73 (2C, N-CH_2-). ESI-TOF-MS: m/z calculated for $C_{20}H_{44}NBr$ $[M\text{-}Br]^+$: 298.35; found: 298.39 $[M\text{-}Br]^+$. Elemental analysis: Calculated for $C_{20}H_{44}NBr$: C, 63.47; H, 11.72; N, 3.70. Found: C, 62.97; H, 11.78; N, 3.61.

Diethyldipropylammonium bromide **(9)**: Method A. Reagents: propyl bromide (7.63 ml, 83.96 mmol), potassium carbonate (11.60 g, 83.96 mmol) and diethyl formamide (50 ml). Reaction temperature 60 °C and reaction time 44 h. Yield (light brown powder) 0.48 g (5%). ^{1}H-NMR ($CDCl_3$, 500 MHz, ppm): 1.04 (6H, t, J = 7.33 Hz, N-$CH_2CH_2CH_3$), 1.37 (6H, t, J = 7.29 Hz, N-CH_2CH_3), 1.77 (4H, m, N-CH_2CH_2-), 3.28 (4H, m, N-CH_2CH_2-), 3.54 (4H, q, J = 7.30 Hz, N-CH_2CH_3). ^{13}C NMR ($CDCl_3$, 126 MHz, ppm): 8.15 (2C, N-CH_2CH_3), 10.90 (2C, N-$CH_2CH_2CH_3$), 15.80 (2C, N-CH_2CH_2-), 54.24 (2C, N-CH_2CH_3), 59.68 (2C, N-CH_2CH_2-). ESI-TOF-MS: m/z calculated for $C_{10}H_{24}NBr$ $[M\text{-}Br]^+$: 158.19; found: 158.17 $[M\text{-}Br]^+$. Elemental analysis: Calculated for $C_{10}H_{24}NBr$: C, 50.42; H, 10.16; N, 5.88. Found: C, 48.62; H, 9.91; N, 5.96.

Diethyldibutylammonium bromide **(10)**: Method A. Reagents: butyl bromide (8.07 ml, 75.12 mmol), potassium carbonate (10.38 g, 75.12 mmol) and diethyl formamide (33 ml). Reaction temperature 80 °C and reaction time 51 h. Yield (brown powder) 1.35 g (14%). ^{1}H-NMR ($CDCl_3$, 500 MHz, ppm): 0.96 (6H, t, J = 7.36 Hz, N-$CH_2CH_2CH_2CH_3$), 1.34 (6H, t, J = 7.26 Hz, N-CH_2CH_3), 1.41 (4H, sextet, J = 7.39 Hz, N-$CH_2CH_2CH_2CH_3$), 1.64 (4H, m, N-CH_2CH_2-), 3.29 (4H, m, N-CH_2CH_2-), 3.49 (4H, q, J = 7.29 Hz, N-CH_2CH_3). ^{13}C NMR ($CDCl_3$, 126 MHz, ppm): 8.09 (2C, N-CH_2CH_3), 13.56 (2C, N-$CH_2CH_2CH_2CH_3$), 19.68 (2C, N-$CH_2CH_2CH_2CH_3$), 23.95 (2C, N-CH_2CH_2-), 54.07 (2C, N-CH_2CH_3), 57.87 (2C, N-CH_2CH_2-). ESI-TOF-MS: m/z calculated for $C_{12}H_{28}NBr$ $[M\text{-}Br]^+$: 186.22; found: 186.19 $[M\text{-}Br]^+$. Elemental analysis: Calculated for $C_{12}H_{28}NBr$: C, 54.13; H, 10.60; N, 5.26. Found: C, 53.14; H, 10.55; N, 5.07.

Diethyldipentylammonium bromide **(11)**: Method D. Reagents: pentyl bromide (9.31 ml, 75.12 mmol), potassium carbonate (10.38 g, 75.12 mmol) and diethyl formamide (34 ml). Reaction temperature 80 °C and reaction time 72 h. Yield (brown partially microcrystalline gel) 30.5 g (31%). ^{1}H-NMR ($CDCl_3$, 500 MHz, ppm): 0.76 (6H, t, J = 6.99 Hz, N-$CH_2CH_2CH_2CH_2CH_3$), 1.23 (14H, m, N-CH_2CH_3 and N-$CH_2CH_2CH_2CH_2CH_3$), 1.55 (4H, m, N-CH_2CH_2-), 3.16 (4H, m, N-CH_2CH_2-), 3.37 (4H, q, J = 7.28 Hz, N-CH_2CH_3). ^{13}C NMR ($CDCl_3$, 126 MHz, ppm): 7.79 (2C, N-CH_2CH_3), 13.43 (2C, N-$CH_2CH_2CH_2CH_2CH_3$), 21.44 (2C, N-CH_2CH_2-), 21.82 and 28.06 (4C, N-$CH_2CH_2CH_2CH_2CH_3$), 53.73 (2C, N-CH_2CH_3), 57.71 (2C, N-CH_2CH_2-). ESI-TOF-MS: m/z calculated for $C_{14}H_{32}NBr$ $[M\text{-}Br]^+$: 214.25; found: 214.23 $[M\text{-}Br]^+$. Elemental analysis: Calculated for $C_{14}H_{32}NBr$: C, 57.13; H, 10.96; N, 4.76. Found: C, 57.22; H, 11.00; N, 4.86.

Diethyldihexylammonium bromide **(12)**: Method A. Reagents: hexyl bromide (8.71 ml, 62.04 mmol), potassium carbonate (8.57 g, 62.04 mmol) and diethyl formamide (35 ml). Reaction temperature 80 °C and reaction time 44 h. Yield (light brown powder) 2.34 g (23%). ^{1}H-NMR ($CDCl_3$, 500 MHz, ppm): 0.87 (6H, t, J = 7.02 Hz, N-$CH_2CH_2CH_2CH_2CH_2CH_3$), 1.33 (18H,

m, N-$CH_2C\mathbf{H}_3$ and N-$CH_2CH_2C\mathbf{H}_2C\mathbf{H}_2CH_2CH_3$), 1.67 (4H, m, N-$CH_2C\mathbf{H}_2$-), 3.28 (4H, m, N-$C\mathbf{H}_2CH_2$-), 3.53 (4H, q, $J = 7.27$ Hz, N-$C\mathbf{H}_2CH_3$). ^{13}C NMR ($CDCl_3$, 126 MHz, ppm): 8.17 (2C, N-$CH_2\mathbf{C}H_3$), 13.78 (2C, N-$CH_2CH_2CH_2CH_2CH_2\mathbf{C}H_3$), 22.10 (2C, N-$CH_2\mathbf{C}H_2$-), 22.33, 26.05 and 31.15 (6C, N-$CH_2CH_2\mathbf{C}H_2\mathbf{C}H_2\mathbf{C}H_2CH_2CH_3$), 54.19 (2C, N-$\mathbf{C}H_2CH_3$), 58.15 (2C, N-$\mathbf{C}H_2CH_2$-). ESI-TOF-MS: m/z calculated for $C_{16}H_{36}NBr$ $[M\text{-}Br]^+$: 242.28; found: 242.31 $[M\text{-}Br]^+$. Elemental analysis: Calculated for $C_{16}H_{36}NBr$: C, 59.61; H, 11.26; N, 4.34. Found: C, 59.12; H, 11.26; N, 4.20.

Diethyldimethylammonium iodide **(13)**: Method E. Reagents: ethyl iodide (7.03 ml, 87.30 mmol), potassium carbonate (12.06 g, 87.30 mmol) and dimethyl formamide (35 ml). Reaction temperature 50 °C and reaction time 48 h. Yield (white powder) 2.43 g (24%). ^{1}H-NMR ($CDCl_3$, 500 MHz, ppm): 1.42 (6H, t, $J = 7.30$ Hz, N-$CH_2C\mathbf{H}_3$), 3.34 (6H, s, N-$C\mathbf{H}_3$), 3.68 (4H, q, $J = 7.31$ Hz, N-$C\mathbf{H}_2CH_3$). ^{13}C NMR ($CDCl_3$, 126 MHz, ppm): 8.65 (2C, N-$CH_2\mathbf{C}H_3$), 50.51 (2C, N-$\mathbf{C}H_3$), 59.36 (2C, N-$\mathbf{C}H_2CH_3$). ESI-TOF-MS: m/z calculated for $C_6H_{16}NI$ $[M\text{-}I]^+$: 102.13; found: 102.10 $[M\text{-}I]^+$. Elemental analysis: Calculated for $C_6H_{16}NI$: C, 31.46; H, 7.04; N, 6.11. Found: C, 31.03; H, 7.14; N, 6.08.

Dimethyldipropylammonium iodide **(14)**. Method E. Reagents: propyl iodide (7.56 ml, 87.30 mmol), potassium carbonate (12.06 g, 87.30 mmol) and dimethyl formamide (30 ml). Reaction temperature 80 °C and reaction time 48 h. Yield (white powder) 2.09 g (21%). ^{1}H-NMR ($CDCl_3$, 500 MHz, ppm): 1.05 (6H, t, $J = 7.31$ Hz, N-$CH_2CH_2C\mathbf{H}_3$), 1.81 (4H, m, N-$CH_2\mathbf{C}H_2CH_3$), 3.37 (6H, s, N-$C\mathbf{H}_3$), 3.53 (4H, m, N-$C\mathbf{H}_2CH_2CH_3$). ^{13}C NMR ($CDCl_3$, 126 MHz, ppm): 10.59 (2C, N-$CH_2CH_2\mathbf{C}H_3$), 16.41 (2C, N-$CH_2\mathbf{C}H_2CH_3$), 51.52 (2C, N-$\mathbf{C}H_3$), 65.81 (2C, N-$\mathbf{C}H_2CH_2CH_3$). ESI-TOF-MS: m/z calculated for $C_8H_{20}NI$ $[M\text{-}I]^+$: 130.16; found: 130.12 $[M\text{-}I]^+$. Elemental analysis: Calculated for $C_8H_{20}NI$: C, 37.37; H, 7.84; N, 5.45. Found: C, 37.17; H, 7.99; N, 5.36.

Dibutyldimethylammonium iodide **(15)**: Method E. Reagents: butyl iodide (7.99 ml, 70.12 mmol), potassium carbonate (9.69 g, 70.12 mmol) and dimethyl formamide (30 ml). Reaction temperature 80 °C and reaction time 48 h. Yield (white powder) 1.96 g (20%). ^{1}H-NMR ($CDCl_3$, 500 MHz, ppm): 1.02 (6H, t, $J = 7.36$ Hz, N-$CH_2CH_2CH_2C\mathbf{H}_3$), 1.45 (4H, sextet, $J = 7.41$ Hz, N-$CH_2CH_2C\mathbf{H}_2CH_3$), 1.72 (4H, m, N-$CH_2C\mathbf{H}_2CH_2CH_3$), 3.37 (6H, s, N-$C\mathbf{H}_3$), 3.54 (4H, m, N-$C\mathbf{H}_2CH_2CH_2CH_3$). ^{13}C NMR ($CDCl_3$, 126 MHz, ppm): 13.69 (2C, N-$CH_2CH_2CH_2\mathbf{C}H_3$), 19.54 (2C, N-$CH_2CH_2\mathbf{C}H_2CH_3$), 24.69 (2C, N-$CH_2\mathbf{C}H_2CH_2CH_3$), 51.47 (2C, N-$\mathbf{C}H_3$), 64.15 (2C, N-$\mathbf{C}H_2CH_2CH_2CH_3$). ESI-TOF-MS: m/z calculated for $C_{10}H_{24}NI$ $[M\text{-}I]^+$: 158.19; found: 158.17 $[M\text{-}I]^+$. Elemental analysis: Calculated for $C_{10}H_{24}NI$: C, 42.11; H, 8.48; N, 4.91. Found: C, 41.99; H, 8.64; N, 4.84.

Dimethyldipentylammonium iodide **(16)**: Method E. Reagents: pentyl iodide (8.34 ml, 63.84 mmol), potassium carbonate (8.82 g, 63.84 mmol) and dimethyl formamide (30 ml). Reaction temperature 80 °C and reaction time 48 h. Yield (white powder) 2.00 g (20%). ^{1}H-NMR ($CDCl_3$, 500 MHz, ppm): 0.90 (6H, t, $J = 6.96$ Hz, N-$CH_2CH_2CH_2CH_2C\mathbf{H}_3$), 1.38 (8H, m, N-$CH_2CH_2(C\mathbf{H}_2)_2CH_3$), 1.72 (4 H, m, N-$CH_2C\mathbf{H}_2CH_2CH_2CH_3$), 3.36 (6 H, s, N-$C\mathbf{H}_3$), 3.53 (4H, N-$C\mathbf{H}_2$-). ^{13}C NMR ($CDCl_3$, 126 MHz, ppm): 13.74 (2C, N-$CH_2CH_2CH_2CH_2\mathbf{C}H_3$), 22.19, 22.45 and 28.11 (6C, N-$CH_2(\mathbf{C}H_2)_3CH_3$), 51.46 (2C, N-$\mathbf{C}H_3$), 64.26 (2C, N-$\mathbf{C}H_2$-). ESI-TOF-MS: m/z calculated for $C_{12}H_{28}NI$ $[M\text{-}I]^+$: 186.22; found: 186.21 $[M\text{-}I]^+$. Elemental analysis: Calculated for $C_{12}H_{28}NI$: C, 46.01; H, 9.01; N, 4.47. Found: C, 45.93; H, 9.14; N, 4.39.

Dimethyldihexylammonium iodide **(17)**: Method E. Reagents: hexyl iodide (8.65 ml, 58.60 mmol), potassium carbonate (8.10 g, 58.60 mmol) and dimethyl formamide (30 ml). Reaction temperature 80 °C and reaction time 48 h. Yield (white sticky powder) 1.74 g (17%). ^{1}H-NMR ($CDCl_3$, 500 MHz, ppm): 0.85 (6H, t, $J = 7.05$ Hz, N-$CH_2CH_2CH_2CH_2CH_2C\mathbf{H}_3$), 1.32 (12H, m, N-$CH_2CH_2(C\mathbf{H}_2)_3CH_3$), 1.69 (4H, m, N-$CH_2C\mathbf{H}_2$-), 3.33 (6H, s, N-$C\mathbf{H}_3$), 3.50 (4H, m, N-$C\mathbf{H}_2$-). ^{13}C NMR ($CDCl_3$, 126 MHz, ppm): 13.81 (2C, N-$CH_2CH_2CH_2CH_2CH_2\mathbf{C}H_3$), 22.73 (2C, N-$CH_2\mathbf{C}H_2$-), 22.31, 25.76 and 31.17 (6C, N-$CH_2CH_2(\mathbf{C}H_2)_3CH_3$), 51.49 (2C, N-$\mathbf{C}H_3$), 64.28 (2C, N-$\mathbf{C}H_2$-). ESI-TOF-MS: m/z calculated for $C_{14}H_{32}NI$ $[M\text{-}I]^+$: 214.25; found: 214.23 $[M\text{-}I]^+$. Elemental analysis: Calculated for $C_{14}H_{32}NI$: C, 49.27; H, 9.45; N, 4.10. Found: C, 49.58; H, 9.73; N, 4.04.

Diethyldipropylammonium iodide **(18)**: Method E. Reagents: propyl iodide (6.82 ml, 70.12 mmol), potassium carbonate (9.69 g, 70.12 mmol) and diethyl formamide (40 ml). Reaction temperature 80 °C and reaction time 48 h. Yield (light yellow powder) 2.79 g (28%). ^{1}H-NMR ($CDCl_3$, 500 MHz, ppm): 1.02 (6H, t, $J = 7.32$ Hz, N-$CH_2CH_2C\mathbf{H}_3$), 1.34 (6H, t, $J = 7.25$ Hz, N-$CH_2C\mathbf{H}_3$), 1.74 (4H, m, N-$CH_2C\mathbf{H}_2$-), 3.26 (4H, m, N-$C\mathbf{H}_2CH_2$-), 3.48 (4H, q, $J = 7.29$ Hz, N-$C\mathbf{H}_2CH_3$). ^{13}C NMR ($CDCl_3$, 126 MHz, ppm): 8.30 (2C, N-$CH_2\mathbf{C}H_3$), 10.82 (2C, N-$CH_2CH_2\mathbf{C}H_3$), 15.84 (2C, N-$CH_2\mathbf{C}H_2$-), 54.34 (2C, N-$\mathbf{C}H_2CH_3$), 59.69 (2C, N-$\mathbf{C}H_2CH_2$-) ESI-TOF-MS: m/z calculated for $C_{10}H_{24}NI$ $[M\text{-}I]^+$: 158.19; found: 158.17 $[M\text{-}I]^+$. Elemental analysis: Calculated for $C_{10}H_{24}NI$: C, 42.11; H, 8.48; N, 4.91. Found: C, 41.26; H, 8.55; N, 4.79.

Diethyldibutylammonium iodide **(19)**: Method E. Reagents: butyl iodide (7.27 ml, 63.84 mmol), potassium carbonate (8.82 g, 63.84 mmol) and diethyl formamide (40 ml). Reaction temperature 80 °C and reaction time 48 h. Yield (light yellow powder) 3.23 g (32%). ^{1}H-NMR ($CDCl_3$, 500 MHz, ppm): 1.00 (6H, t, $J = 7.36$ Hz, N-$CH_2CH_2CH_2C\mathbf{H}_3$), 1.38 (6H, t, $J = 7.26$ Hz, N-$CH_2\mathbf{C}H_3$), 1.46 (4H, sextet, $J = 7.39$ Hz, N-CH_2CH_2

CH_2CH_3), 1.69 (4H, m, N-CH_2CH_2-), 3.31 (4H, m, N-CH_2CH_2-), 3.50 (4H, q, $J = 7.29$ Hz, N-CH_2CH_3). ^{13}C NMR ($CDCl_3$, 126 MHz, ppm): 8.37 (2C, N-CH_2CH_3), 13.66 (2C, N-$CH_2CH_2CH_2CH_3$), 19.76 (2C, N-$CH_2CH_2CH_2CH_3$), 24.14 (2C, N-CH_2CH_2-), 54.38 (2C, N-CH_2CH_3), 58.14 (2C, N-CH_2CH_2-). ESI-TOF-MS: m/z calculated for $C_{12}H_{28}NI$ $[M\text{-}I]^+$: 186.22; found: 186.21 $[M\text{-}I]^+$. Elemental analysis: Calculated for $C_{12}H_{28}NI$: C, 46.01; H, 9.01; N, 4.47. Found: C, 45.49; H, 9.11; N, 4.41.

Diethyldipentylammonium iodide **(20)**: Method E. Reagents: pentyl iodide (7.65 ml, 58.60 mmol), potassium carbonate (8.10 g, 58.60 mmol) and diethyl formamide (35 ml). Reaction temperature 80 °C and reaction time 48 h. Yield (light yellow powder) 3.53 g (35%). ^{1}H-NMR ($CDCl_3$, 500 MHz, ppm): 0.87 (6H, t, $J = 6.95$ Hz, N-$CH_2CH_2CH_2CH_2CH_3$), 1.34 (14H, m, N-CH_2CH_3 and N-$CH_2CH_2CH_2CH_2CH_3$), 1.66 (4H, m, N-CH_2CH_2-), 3.26 (4H, m, N-CH_2CH_2-), 3.46 (4H, q, $J = 7.28$ Hz, N-CH_2CH_3). ^{13}C NMR ($CDCl_3$, 126 MHz, ppm): 8.24 (2C, N-CH_2CH_3), 13.66 (2C, N-$CH_2CH_2CH_2CH_2CH_3$), 21.80 (2C, N-CH_2CH_2-), 22.06 and 28.27 (4C, N-$CH_2CH_2CH_2CH_2CH_3$), 54.22 (2C, N-CH_2CH_3), 58.15 (2C, N-CH_2CH_2-). ESI-TOF-MS: m/z calculated for $C_{14}H_{32}NI$ $[M\text{-}I]^+$: 214.25; found: 214.25 $[M\text{-}I]^+$. Elemental analysis: Calculated for $C_{14}H_{32}NI$: C, 49.27; H, 9.45; N, 4.10. Found: C, 49.01; H, 9.56; N, 4.02.

Diethyldihexylammonium iodide **(21)**: Method E. Reagents: hexyl iodide (7.99 ml, 54.15 mmol), potassium carbonate (7.48 g, 54.15 mmol) and diethyl formamide (35 ml). Reaction temperature 80 °C and reaction time 48 h. Yield (light yellow powder) 2.55 g (26%). ^{1}H-NMR ($CDCl_3$, 500 MHz, ppm): 0.84 (6H, t, $J = 7.03$ Hz, N-$CH_2CH_2CH_2CH_2CH_2CH_3$), 1.31 (18H, m, N-CH_2CH_3 and N-$CH_2CH_2CH_2CH_2CH_2CH_3$), 1.65 (4H, m, N-CH_2CH_2-), 3.26 (4H, m, N-CH_2CH_2-), 3.46 (4H, q, $J = 7.28$ Hz, N-CH_2CH_3). ^{13}C NMR ($CDCl_3$, 126 MHz, ppm): 8.25 (2C, N-CH_2CH_3), 13.71 (2C, N-$CH_2CH_2CH_2CH_2CH_2CH_3$), 22.08 (2C, N-CH_2CH_2-), 22.24, 25.92 and 31.03 (6C, N-$CH_2CH_2CH_2CH_2CH_2CH_3$), 54.25 (2C, N-CH_2CH_3), 58.17 (2C, N-CH_2CH_2-). ESI-TOF-MS: m/z calculated for $C_{16}H_{36}NI$ $[M\text{-}I]^+$: 242.28; found: 242.28 $[M\text{-}I]^+$. Elemental analysis: Calculated for $C_{16}H_{36}NI$: C, 52.03; H, 9.82; N, 3.79. Found: C, 51.69; H, 9.92; N, 3.76.

2.2. Characterization in liquid state

The formation of QA halides were confirmed by ^{1}H and ^{13}C NMR and also by ESI TOF MS. ^{1}H-NMR spectra and ^{13}C-NMR spectra were measured in $CDCl_3$ at 30 °C by using a Bruker Avance DRX 500 NMR spectrometer operating at 500 MHz for ^{1}H and 126 MHz for ^{13}C. Electrospray mass spectrometric measurements were obtained by using the Micromass LCT time-of-flight (TOF) mass spectrometer with electrospray ionization (ESI). All the compounds were measured by using positive mode with sample concentration of 25 mg/L in methanol solution. The elemental analyses were carried out with Vario EL III CHN elemental analyser by using sample weights of 3–5 mg.

2.3. Structure analysis

The X-ray structures for compounds **2**, **9**, **18** and **19** were determined by X-ray single crystal diffraction. Colourless single crystals were obtained by recrystallization from MeOH/EtAc solution. The crystallographic data was recorded with a Nonius KappaCCD diffractometer at −100 °C using graphite monochromaticed Mo$K\alpha$ ($\lambda = 0.71069$ Å) radiation. The data was processed with EvalCCD [70] software package and the absorption correction was performed using SADABS (included in EvalCCD software package). All the structures were solved with direct methods (SIR92 [71], SIR97 [72], SIR2002 [73] or SHELXS-97 [74]) and refined on F^2 by full-matrix least-squares techniques (SHELXL-97 [75]) by using anisotropic temperature factors. All the hydrogen atoms were calculated to their ideal positions as riding atoms by using isotropic temperature factors.

2.4. X-ray powder diffraction analyses

The powder diffraction data of **1**–**21** were measured to investigate the crystallinity of the compounds and in case of compounds **2**, **9**, **18** and **19** the powder diffraction data was used to confirm the expected similarities between the single crystals and the microcrystalline bulk material. The calculated powder data were obtained from the structural parameters of each of the compounds by DIAMOND 3.0b software package [76]. X-ray powder diffraction data were obtained at room temperature by Huber G670 imaging-plate Guinier camera. The sealed-tube X-ray generator system was operated at 45 kV and 25 mA and pure line-focused Cu$K\alpha_1$ radiation ($\lambda = 1.5406$ Å) was produced by primary beam curved germanium monochromator ($d = 3.266$ Å). The measurements were carried out in Guinier-type transmission geometry with the angle of incidence 45° to the sample normal. The handground samples were prepared on the vaseline-coated Mylar foil of 3.5 μm thickness. The diffracted X-ray photons with the angular range of 4–100° (2θ) were captured to the curved imaging plate detector and the diffraction data was recorded with step resolution of 0.005 (2θ).

2.5. Thermal properties

Melting points of the compounds were determined on PerkinElmer PYRIS Diamond DSC. Some of the melting points were also confirmed with Mettler Toledo

FP62 melting point instrument (not corrected) to support the interpretation of DSC curves. DSC measurements were carried out using 50 μl sealed aluminium sample pans with pinholes. The temperature calibration was carried out using three standard materials (*n*-decane, In, Zn) and the energy calibration by indium standard. The samples were heated under nitrogen (flow rate of 50 ml/min) with the rate of 10 °C/min from −50 °C close to the predetermined (DSC, TG/DTA) decomposition temperature of each compound. The sample weights used in the measurements were about 4–7 mg.

The thermal decomposition paths were obtained with PerkinElmer Diamond TG/DTA. Measurements were carried out using platinum pans under synthetic air atmosphere (flow rate of 110 mL/min) at temperature range 22–400 °C (heating rate of 10 °C/min). The temperature calibration of the TG/DTA equipment was carried out using melting points of five reference materials (In, Sn, Zn, Al, Au). The weight balance was calibrated by measuring the standard weight as function of temperature. The sample weights used in the measurements were from 5 to 20 mg.

3. Results and discussion

3.1. Characterization in liquid and solid state

The formation of quaternary alkyl ammonium halides was verified with ^{1}H-NMR and ^{13}C-NMR spectroscopy. Mass spectroscopy studies and elemental analysis confirmed the formation of the desired compounds. All the compounds were free of reaction solvents and other impurities based on NMR, MS, elemental analysis and TG/DTA studies. The smallest QA bromides were very hygroscopic, which caused some difficulties in sample preparation for elemental analysis and DSC measurements.

3.2. X-ray structure analysis

Several crystallization attempts were made to produce measurable single crystals of the presented compounds. Various solvents and crystallization conditions were tried but only the compounds **2**, **9**, **18** and **19** recrystallized as single crystals. Compound **2** (dimethyldipropylammonium bromide) crystallized in trigonal space group *P*-3. The asymmetric unit comprises of three unique ion-pairs of **2** (Fig. 1(a) and (b) [76]). Two of the cations are approximately in the same conformation while the conformation of the third cation differs only in the orientation of the terminal ethyl group of one propyl chain. The packing mode reveals that the nonpolar propyl chains of six cations gather together to form disk shaped building blocks, in which the methyl end groups of the propyl chains are pointing inside. These disks are further stacked together to form hydrophobic pillar like regions running through the crystals along the crystallographic *c*-axis (Fig. 1(c)).

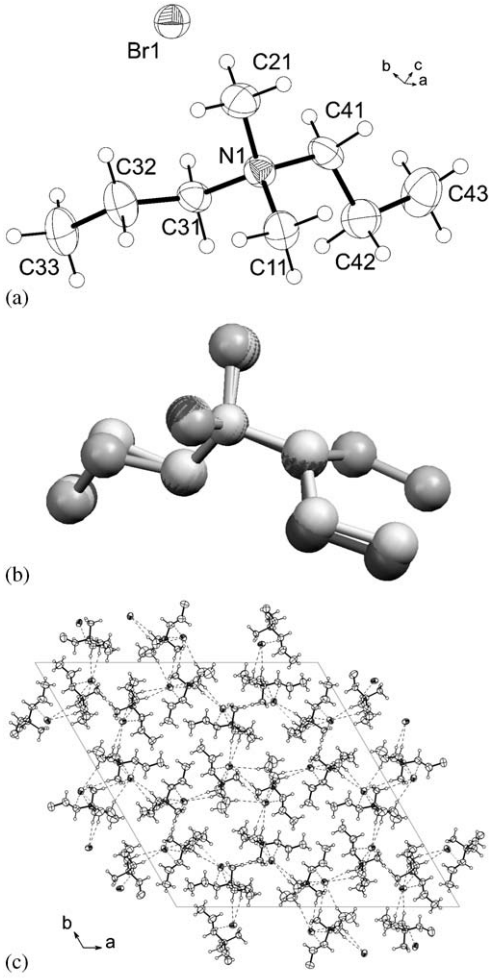

Fig. 1. (a) One of the three ion-pairs in the asymmetric unit of crystal structure of **2** (Thermal ellipsoids are presented at 50% probability level in all figures). (b) A superimposed picture of the three cations in the asymmetric unit showing the variation of the propyl group orientation between the ion pairs. Hydrogen atoms are omitted for clarity. (c) Packing of **2** along the crystallographic *c*-axis with hydrogen bonding ($Br^{-}\cdots H–C < 3.0$ Å) shown as dashed lines. The shortest anion/cation ($Br^{-}\cdots C–N^{+}$) distances are 3.64–3.88 Å and the distance of the bromide anion to the nearest nitrogen ($Br^{-}\cdots N^{+}$) atom is about 4.08(1) Å.

Compound **9**, with a formamide-originating methyl groups replaced by an ethyl, crystallized in monoclinic space group $P2_1/n$. The asymmetric unit of **9** comprises of two conformationally unique cations that differ somewhat in the orientation of the alkyl chains. One of the two ion-pairs and the packing mode is presented in Fig. 2 [76]. As can be seen from Fig. 2b, there are no clear nonpolar areas like pillars or layers formed due to the alkyl chain packing and hydrophobic interactions.

The polar and nonpolar areas are more or less evenly distributed throughout the crystal.

In compound **18** the bromide anion of **9** was changed to larger and generally weaker hydrogen bonding iodide anion. Despite of an initial expectation, **9** and **18** do not have isomorphous structures, as **9** crystallize in monoclinic symmetry whereas **18** crystallize in trigonal space group *R*-3*c*. The structure of **18** has high symmetry and the asymmetric unit is formed only of a half ion-pair (Fig. 3). The compound has a star-like packing when viewed along the crystallographic *c*-axis. The star comprises of six ion pairs of compound **18** so that every other ion pair has the two ethyl groups pointing inwards while every other ion pair has one of its propyl groups pointing to the center of the star. The six ion pairs that form the star are not in the same plane formed by the *a*- and *b*-axis but are interlocked so that every other ion pair is shifted a little along the *c*-axes. The three ion pairs that have ethyl groups at the center form one layer that is interlocked with the other layer, which is formed by the three ion pairs having one propyl group pointing at the center. These layers are further stacked to build up star like pillars along the *c*-axis. Each of the stars is surrounded by three other stars so that two of the six ion pairs forming each star are shared with the adjacent star. The ion pair and the packing mode of **18** can be seen in Fig. 3 [76]. The cause for crystallization of corresponding bromide and iodide salts in a different crystal symmetry is not obvious. Most probably the larger size and thus larger charge distribution of iodide effects the polar interactions and hydrogen bonding between the cation and anion so that the bromide and iodide salts have different energetic minimums and different packing in solid state.

Compound **19** crystallizes in *C*-centred monoclinic space group *C*2/*c*. Like in the structure **18** the

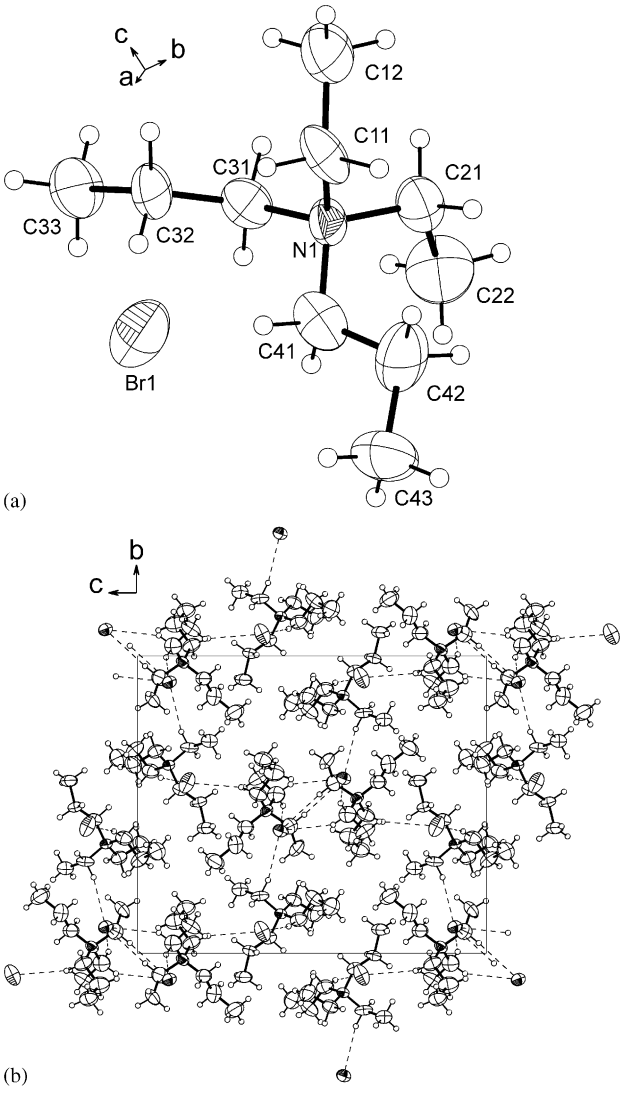

Fig. 2. (a) The ion-pair ordering and molecular structure of **9**. (b) Crystal packing viewed down the *c*-axis with hydrogen bonding ($Br^{-}\cdots H–C < 3.0$ Å) shown as dashed lines. The shortest cation/anion distances are Br1…C41 3.73(33), Br1…C31 3.77(8), and Br1…C21 3.87(26) Å. The distance from bromide to the adjacent nitrogen atoms is 4.47(19) Å.

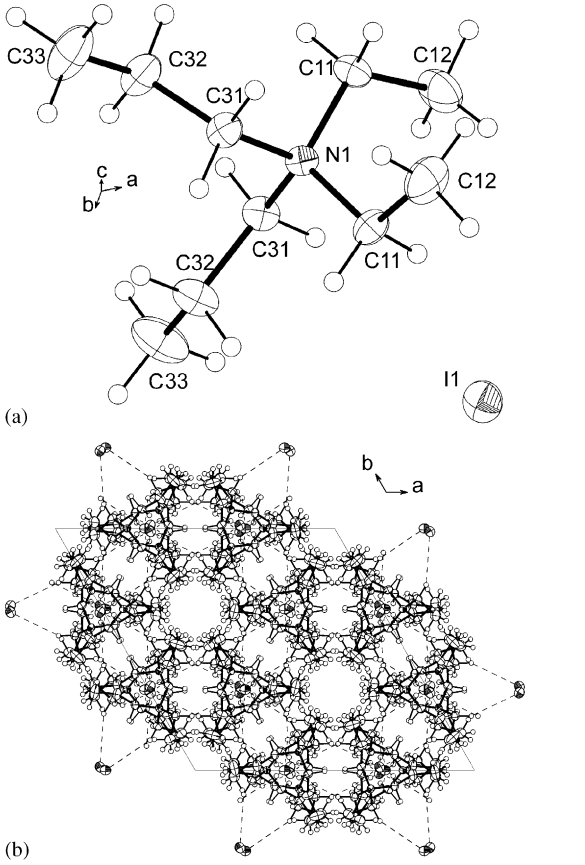

Fig. 3. (a) The ion-pair ordering and numbering scheme of **18** with the packing mode (b). The hydrogen bonds ($I^{-}\cdots H–C < 3.2$ Å) are shown as dashed lines. The shortest cation/anion distances are ($I^{-}\cdots C–N^{+}$) 4.04–4.15 Å and the distance to the adjacent nitrogen atoms is about 4.71(1) Å.

asymmetric unit is described with only a half of one ion-pair. Each anion is surrounded by five cations, the closest CH…I^- distances being about 4 Å. The molecular structure, packing of the ion-pairs and hydrogen bonding of **19** are presented in Fig. 4 [76]. Crystallographic data and the selected bond lengths and angles of all four structures are presented in Tables 1 and 2.

3.3. Powder diffraction analysis

The experimental powder data of compounds **1–21** are presented in Fig. 5. The crystallinity of **1–3**, **9–10**, **12–16** and **18–21** was relatively high as quite narrow half-widths of the diffraction peaks with high overall intensity gains were observed. Compounds **4–5** and **11** were partially microcrystalline gels and compounds **7–8** microcrystalline gels, which can be seen from amorphous halo in baseline underneath of the main diffraction peaks. The compound **6** stayed as viscous gel despite of several attempts to solidify it. Thus, only amorphous halo was seen in powder diffraction pattern. The compound **17** existed as sticky powder giving also amorphous halo underneath the main peaks in powder diffraction baseline. The measured powder diffraction data also confirmed the structural similarities of the single crystals and the microcrystalline bulk material in case of compounds **2**, **9**, **18** and **19** as can be seen from Fig. 6.

3.4. Thermal properties

Results of the thermal analyses for compounds **1–21** are presented in Table 3. All the transition temperatures were taken from the peak onsets. Analogous melting

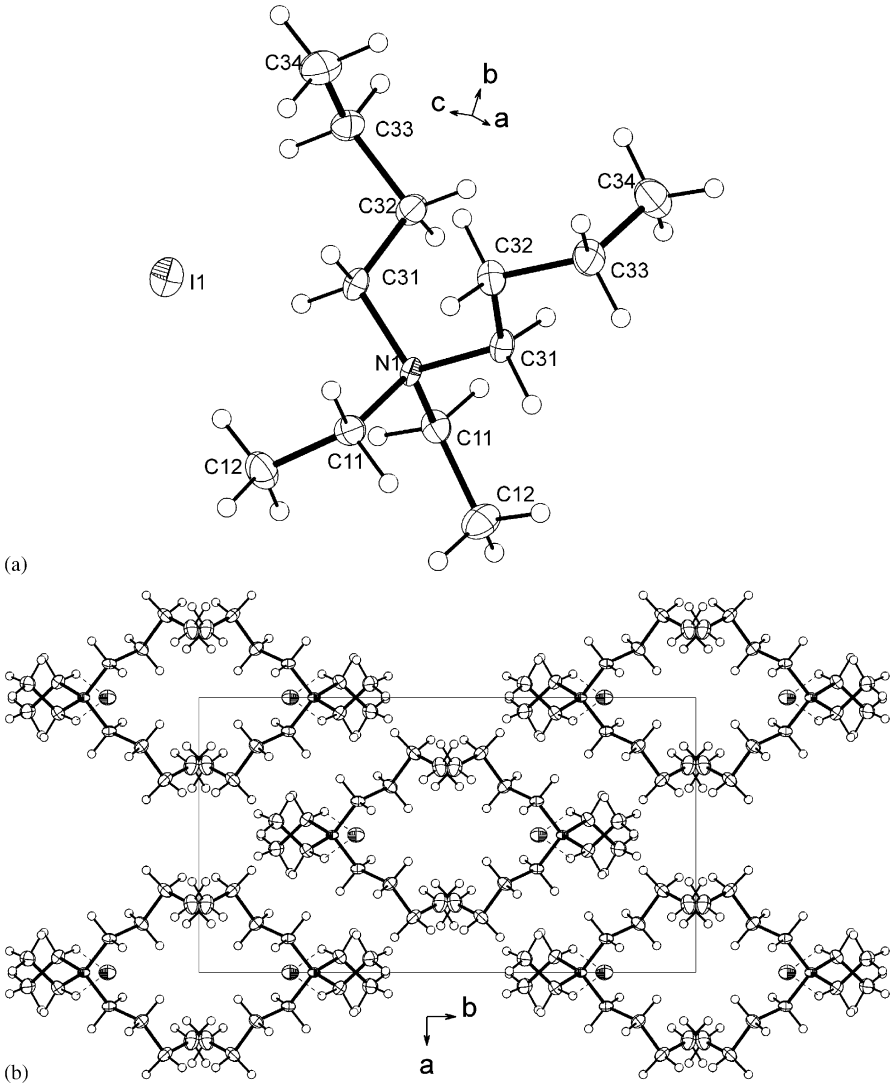

Fig. 4. (a) The ion pair ordering of compound **19**. (b) The packing of the ion pairs with hydrogen bonding ($I^- \cdots H–C < 3.2$ Å) shown as dashed lines. The shortest cation/anion distances are I1…C11 3.97(2), I1…C12 4.09(2) and I1…C31 4.15(1) Å. The distance from bromide to the adjacent nitrogen atoms is about 4.78(1) Å.

Table 1
Crystallographic data for compounds **2**, **9**, **18** and **19**

Compound	**2**	**9**	**18**	**19**
Formula	$C_8H_{20}NBr$	$C_{10}H_{24}NBr$	$C_{10}H_{24}NI$	$C_{12}H_{28}NI$
M_r (g mol^{-1})	210.16	476.42	285.20	313.25
Crystal system	Trigonal	Monoclinic	Trigonal	Monoclinic
Space group	*P*-3	$P2_1/n$	*R*-3*c*	*C*2/*c*
A (Å)	27.241(4)	8.491(13)	16.035(2)	9.2797(19)
B (Å)	27.241(4)	15.645(6)	16.035(2)	16.654(3)
C (Å)	7.8671(16)	18.346(18)	26.849(5)	9.4252(19)
α (deg)	90	90	90	90
β (deg)	90	91.7(2)	90	96.09(3)
γ (deg)	120	90	120	90
V (Å^3)	5055.7(15)	2436(4)	5978.9(17)	1448.4(5)
Z	18	8	18	4
ρ_{calcd} (g/cm^3)	1.242	1.299	1.426	1.437
μ (mm^{-1})	3.604	3.333	2.372	2.183
F (000)	1980	1008	2592	640
Crystal size (mm)	0.4 × 0.3 × 0.25	0.15 × 0.05 × 0.05	0.25 × 0.20 × 0.10	0.25 × 0.15 × 0.10
θ range (deg)	2.59–27.46	3.42–25.07	3.30–24.98	3.17–27.50
Reflections collected	42875	34401	41024	5115
Independent reflections	7718	4301	1155	1653
Data/restraints/parameters	7718/0/272	4301/0/218	1155/0/57	1653/0/66
GooF	1.205	1.040	1.075	1.031
R(int)	0.0782	0.2362	0.0509	0.0361
Final *R* indices ($I>2\sigma(I)$), R_1/wR_2	0.0521/0.0941	0.0934/0.2191	0.0202/0.0391	0.0291/0.0449
R indices (all data), R_1/wR_2	0.0813/0.1005	0.2176/0.2738	0.0262/0.0411	0.0491/0.0480
Largest diff. peak/hole (e/Å^3)	0.918/−0.714	1.039/−0.524	0.507/−0.283	0.373/−0.503

Table 2
Selected bond lengths (Å) and bond angles (deg) of compounds **2**, **9**, **18** and **19**

Compound	**2**	**9**	**18**	**19**
N(1)–C(11)	1.504(5)	1.525(13)	1.521(2)	1.521(3)
N(1)–C(21)	1.503(6)	1.505(12)	1.521(2)	1.521(3)
N(1)–C(31)	1.518(5)	1.494(13)	1.513(2)	1.516(3)
N(1)–C(41)	1.523(6)	1.503(14)	1.513(2)	1.516(3)
C(11)–N(1)–C(21)	109.2(4)	106.7(8)	111.7(2)	111.1(2)
C(11)–N(1)–C(31)	110.8(3)	110.2(8)	108.5(1)	108.9(1)
C(11)–N(1)–C(41)	110.0(3)	108.2(8)	108.0(1)	108.4(1)
C(21)–N(1)–C(31)	110.4(3)	110.2(8)	108.0(2)	108.4(1)
C(21)–N(1)–C(41)	106.9(3)	112.4(8)	108.5(1)	108.9(1)
C(31)–N(1)–C(41)	109.5(3)	109.0(8)	112.2(2)	111.2(2)

transitions were also observed on TG/DTA measurements, which are presented in Figs. 7 and 8. Melting points (T_m) were also monitored by Melting point apparatus to support the interpretation of DSC scans especially in cases where it turned out that the compound exhibited only solid–solid phase transitions instead of melting prior to thermal decomposition. The comparison of the observed melting points and the melting points of analogous tetraalkylammonium bromides and iodides is presented in Fig. 9. Only one of the DSC measurements is presented in Fig. 10, since they were in most cases analogous to DTA scans. It should also be noted that the DSC scans were always started from −50 °C. Thus, some low temperature transitions are not visible on DTA as the TG/DTA measurements were started from room temperature.

No melting transition was observed on compounds **1**, **9**, **13** and **18** before their thermal decomposition. In case of the **2**, **10** and **19** the T_m was observed either during or just before a start of thermal decomposition (Figs. 7 and 8). However, preceding six compounds manifested one or two solid–solid phase-transitions prior to decomposition as can be seen in Table 3. The thermal decomposition started generally between 210 and 235 °C with exception of **13**, which decomposition started at 310 °C. In all cases decomposition occurred without identifiable cleavages and was ended by reaching a zero weight generally before 360 °C.

The dimethyldipropylammonium bromide (**2**) showed one (occasionally two) solid–solid phase-transitions at 42.9 or 98.1 °C following with T_m at 225.4 °C just before decomposition. Depending on the purity and the crystallization conditions of the compound, it occasionally solidified either as mixture of two different polymorphs or as one of the polymorphs. On detailed studies it was found out that, even small residuals of alkaline metal halide, water, or solvent affected to the result of crystallization. Based on the powder diffraction measurements, the reported single crystal structure at low temperature and one of the room temperature

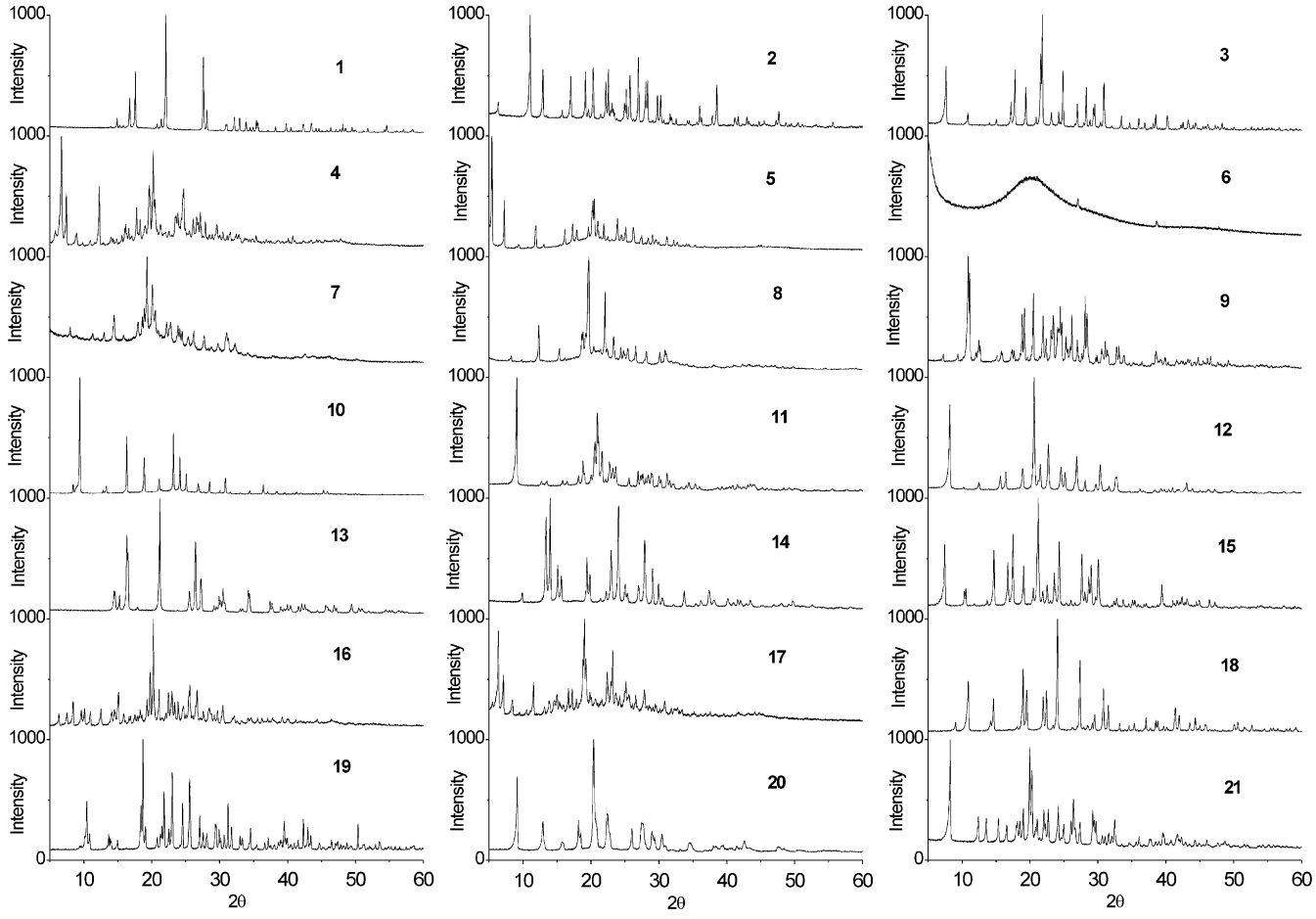

Fig. 5. Experimental powder data of compounds **1–21**.

polymorphs were analogous to each other. Unfortunately, the other room temperature polymorph was not being able to solve from the measured powder data. The dimethyldibutylammonium bromide (**3**) showed two solid–solid phase-transitions at 68.3 °C and 91.8 °C following with T_m at 155.5 °C; hence, having isotropic liquid range of about 70 °C (Fig. 10). In the case of dimethyldipentylammonium bromide (**4**) the T_m was observed at 76.2 °C being about 80 °C lower than on compound **3** thereby extending the liquid range up to ~140 °C. In case of the dimethyldihexylammonium bromide (**5**) the T_m was observed at 53.9 °C and finally no clear melting transition was observed for dimethyldiheptylammonium bromide (**6**). With more detailed DSC scans of compound **6** only very weak endothermic transition (4.4 J/g) was observed in some cases during the second heating at 38.8 °C. The transition may be stated as melting transition of the weakly crystallized proportion of the compound as compound **6** showed to be microcrystalline viscose gel. Several attempts were made to solidify (crystallization and extended drying experiments) the compound but in all cases it remained as viscose gel.

The decreasing trend of T_m was also observed for dimethyldialkylammonium iodides (**14–17**) from 175.6 to 45.1 °C and on diethyldialkylammonium iodides (**19–21**) from 207.7° to 72.6°. Similar behaviour is also known for the tetraalkylammonium bromides and iodides [77–79], when the alkyl chain lengths are increased, as can be seen from Table 3 and Fig. 9.

In case of the diethyldialkylammonium bromides (**9–12**) decreasing trend is not as obvious as only two of the four compounds exhibited T_m. In addition, compound **11** showed somewhat lower T_m (57.5 °C) than it would have been expected as clearly higher T_m (74.6°) was observed on compound **12** with longer alkyl chains. The physical nature (gel) of the compound **11** was quite similar to **6** and as a consequence, the observed melting transition was very broad effecting substantially to the observed T_m onset. One potential explanation is that some solvent or water residuals still hindered proper crystallization of this compound.

The DSC scans of compounds **7–8** were quite complicated to analyse as several weak endothermic (and/or exothermic) transitions were observed. Further drying and crystallization attempts were carried out also

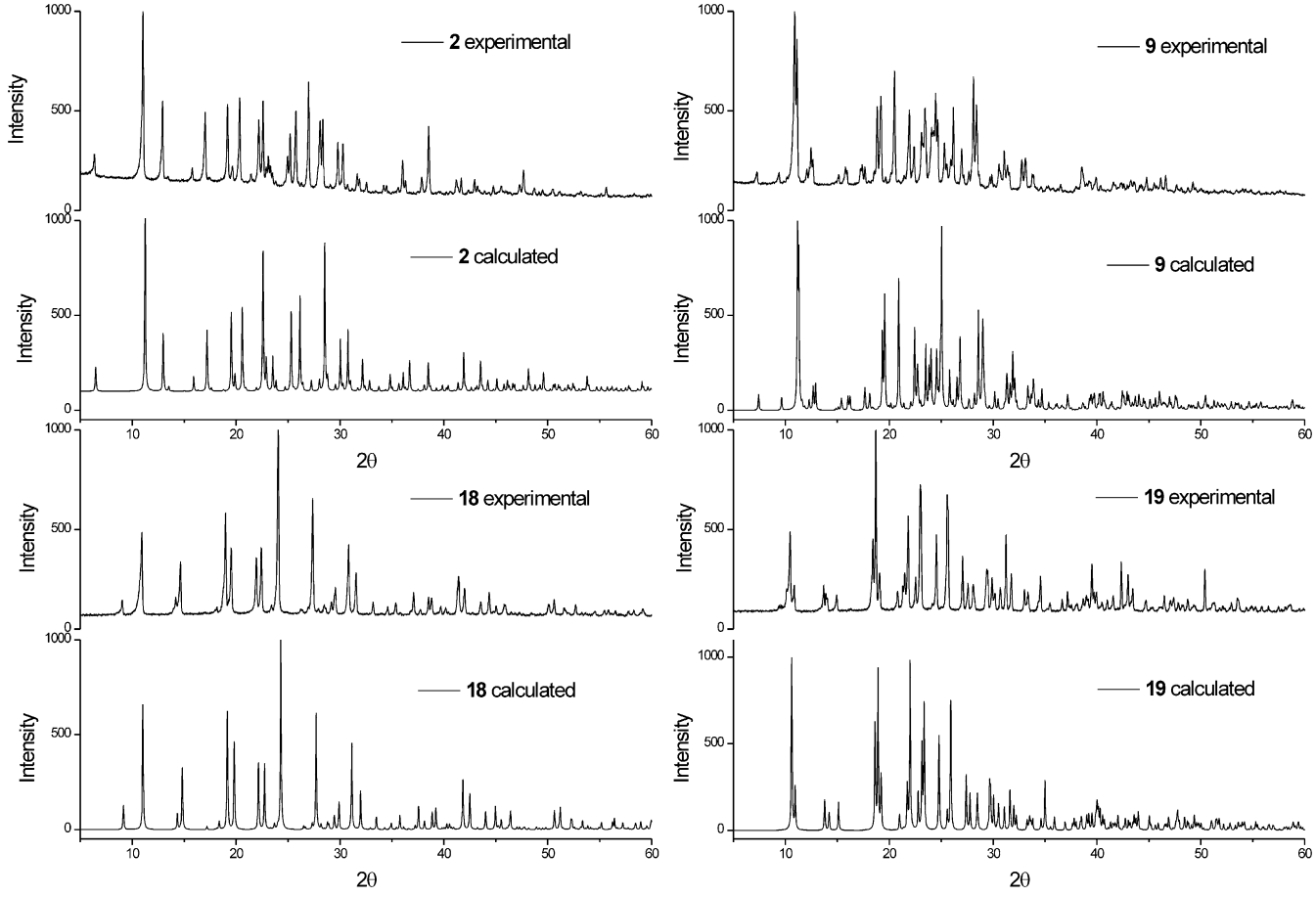

Fig. 6. Experimental powder data of **2**, **9**, **18** and **19** compared with calculated data, which were obtained from the single crystal structure parameters.

Table 3
Phase-transition temperatures (DSC onsets), melting points (DSC onsets) and enthalpy changes and decomposition ranges for compounds **1–21**

Compound	T_{pt} and enthaply change (°C, (J/g))	T_m and enthalpy change (°C, (J/g))	Decomposition range (°C)
1	48.4 (45.1)		230–320
2[b]	(42.9 (45.7)) 98.1 (16.1)	225.4[a]	230–310
3	68.3 (17.4), 91.8 (14.5)	155.5 (31.5)	225–315
4		76.2 (31.1)	220–305
5		53.9 (26.0)	215–320
6[c]			220–360
7[c]			210–305
8[c]			215–320
9	31.2 (5.0), 96.3 (29.9)		235–330
10	−14.6 (9.2), 6.2 (6.6)	197.8[a]	210–320
11		57.5 (18.0)	205–365
12	−15.1 (5.2)	74.6 (79.1)	200–310
13	71.8 (44.5)		310–345
14		175.6 (48.9)	235–320
15	102.5 (12.2)	142.7 (44.4)	235–310
16		86.4 (39.2)	230–325
17		45.1 (20.3)	225–335
18	57.6 (21.7), 101.3 (4.6)		250–325
19	57.6 (67.7)	207.7[a]	220–310
20	66.6 (29.7)	94.8 (23.4)	215–340
21		72.6 (66.2)	220–340

[a]Only onset value can be determined (TG/DTA) as the melting is severely overlapped with decomposition.
[b]Two different polymorphs (see text).
[c]See text.

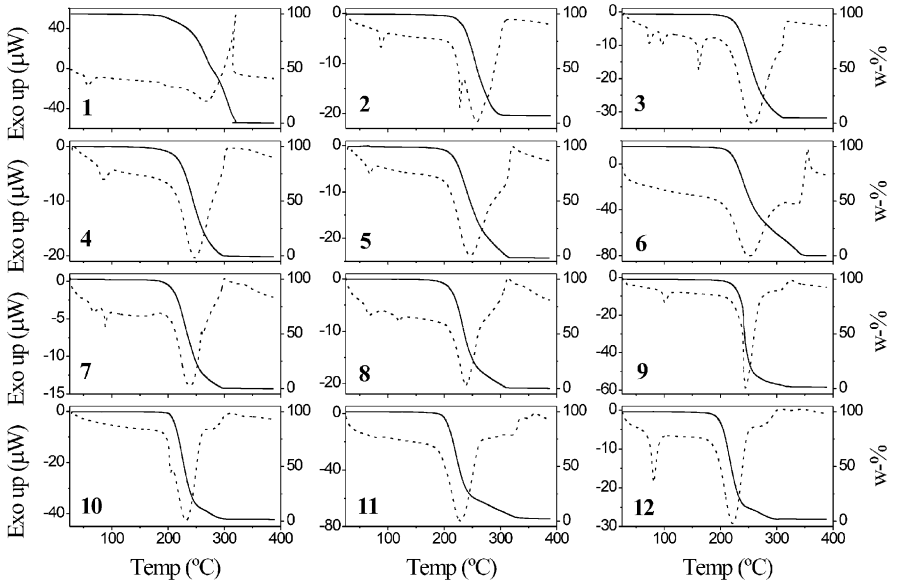

Fig. 7. TG (straight line) and DTA (dash line) curves for QA bromides (compounds **1–12**). The exothermic events are pointing up in DTA curves.

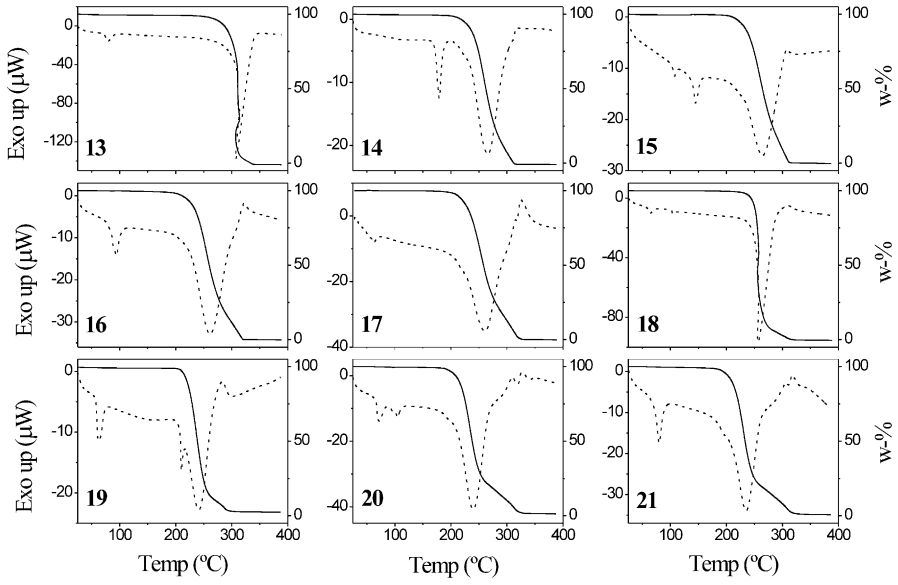

Fig. 8. TG (straight line) and DTA (dash line) curves for QA iodides (compounds **13–21**). The exothermic events are pointing up in DTA curves.

for these two compounds without success. The highest endothermic transition occurred for both compounds close to 60 °C suggesting that as the alkyl chain lengths increase further on, the longer alkyl chains start to enhance the crystallization properties. That is also reported by Godlewska et al. [80] and Alami et al. [81] which studied various dialkyldimethylammonium halides with at least 12 carbons in longer alkyl chains. These compounds started to exhibit liquid crystalline properties around 60–90 °C having the clearing point as high as around 150 °C. Appearing of liquid crystalline phases for compounds **7–8** cannot be ruled out as several subsequent endothermic transitions were observed in DSC scans. Unambiguous interpretation of these phase transitions needs the polarizing optical thermoscopy, which is out of the scope of this study; therefore, the final characterization of these transitions is left to the future studies. However, the liquid range of at least 120–130 °C can be estimated for **7–8** as these two compounds are more or less gels already at room temperature and since the last transition was observed roughly at 60 °C.

Similar wide liquid ranges (120–180 °C) were also observed for compounds **4–5**, **11–12**, **16–17** and **20–21**,

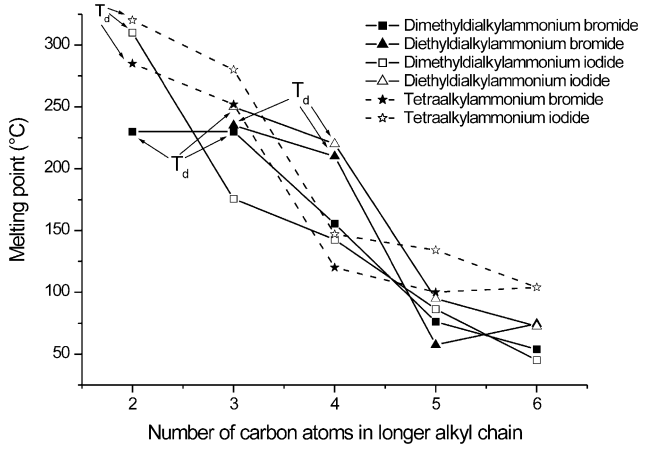

Fig. 9. The melting points of compounds **1–5** and **9–21** as a function of number of carbon atoms in longer alkyl chain. The T_m of tetraalkylammonium bromides and iodides [75–77] are also added for comparison of results. For compounds **1–2**, **9–10**, **13**, **18–19**, tetraethylammonium bromide and iodide instead of T_m the thermal decomposition temperature (extrapolated onset), T_d, is presented as these compounds decompose before or during melting.

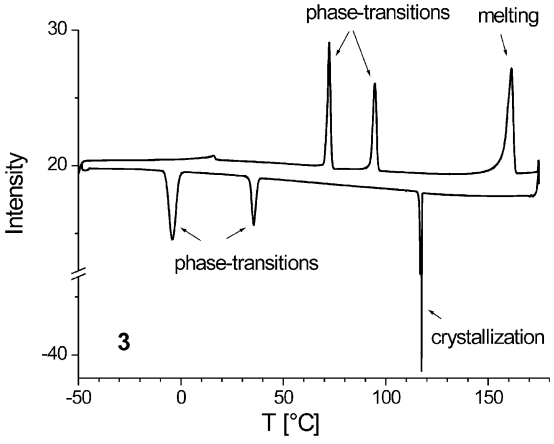

Fig. 10. The DSC curve of compound **3** as an example of DSC measurements. The upper curve represents the heating scan and the lower curve the cooling scan.

all having 5–6 carbon atoms in alkyl chains. The melting points of these compounds showed to be relatively low (varying from 45 to 95 °C) and their thermal decomposition started generally at temperature range of 200–230 °C (no identifiable cleavages). Liquid ranges of about 60 °C and 90 °C were also observed for **14** and **15** but melting points for these compounds were rather high being at 175.6 and 142.7 °C, respectively. Finally, for compounds **12**, **15** and **20** one solid–solid phase-transition was observed before melting at −15.1, 102.5 and 66.6 °C, respectively. The phase transition signals were also observed on cooling scans typically showing slight hysteresis. Additionally, sharp crystallization transitions were observed for compounds having highest crystallinity. Substantially broader transition signals were obtained as the crystallinity of compounds decreased, disappearing completely for compounds appearing as viscose gels.

4. Conclusions

Twenty-one $R_2R'_2N^+X^-$-type QA halides were synthesized by using a simple synthetic route wherein the dimethyl- or diethylformamide is reacted with selected alkyl halide in presence of potassium or sodium carbonate. The physical form of the compounds varied from crystalline powders (**2–3**, **9–10**, **12–16**, **18–21**) via sticky powders (**1**, **17**) to microcrystalline gels (**4–8, 11**). The powder diffraction data were measured to investigate the crystalline content of the compounds. The crystal structures of four compounds (**2**, **9**, **18** and **19**) were solved using X-ray single crystal diffraction and their structural similarities with microcrystalline bulk material were confirmed by the powder diffraction data. In spite of several attempts and experiments with several different solvent systems, we were not able to recrystallize the other compounds. Crystallized compounds **9** and **18** (diethyldipropyl ammonium bromide and iodide) did not crystallize in isomorphous structures as might have been expected, probably because of the larger size of the iodide anion that contributes to the polar interactions and hydrogen bonding between the cation and anion thereupon causing different energetic minimums and different packing in solid state.

The thermal analysis showed that the smallest compounds started to decompose before or during melting, therefore no liquid range was observed. When the alkyl chain length was increased the decreasing effect of melting points was observed at same time. The best ionic liquid properties were observed for compounds with 5–6 carbon atoms in alkyl chain. The lowest observed melting points varied between 45 and 95 °C and the compounds remained liquid over a wide temperature range (120–180 °C) prior to decomposition. The wide liquid range enables the potential applicability of these compounds as ionic liquids. Ionic liquid characteristics can also be adjusted by changing the anion, which will be tested in further studies.

The presented small QA halides are also interesting molecules for complexation studies of resorcinarenes as the electron rich resorcinarene cavity is known to complex alkyl ammonium cations via cation–π interactions [23–27]. Resorcinarenes have been shown to form hydrogen bonded molecular capsules [26,27], open wave-like structures and even molecular tubes [82] via self-assembling with the aid of alkyl ammonium cations as the size, shape and charge of the cation is varied. Two wave-like solid state assemblies of these compounds with resorcinarene have already been characterized; a

complex of C-methyl resorcin[4]arene with dimethyldipropyl-ammonium bromide and a complex of Ethyl resorcin[4]arene with dimethyldibutylammonium bromide, and further studies are underway.

5. Supporting information available

Crystallographic data for the structures reported in this paper have been deposited with the Cambridge Crystallographic Data Centre as supplementary publication no. CCDC_244861–244864. Copies of the data can be obtained free of charge on application to CCDC, 12 Union Road, Cambridge CB2 1EZ, UK (fax: (44) 1223 336-033; e-mail: deposit@ccdc.cam.ac.uk).

Acknowledgments

We thank Mr. Reijo Kauppinen and Prof. Erkki Kolehmainen for measuring the NMR spectra and Ms. Elina Hautakangas for measuring the elemental analysis data. K.R. gratefully acknowledges the financial support by the National Technology Agency (TEKES, proj. no. 40004/01) and S.B. correspondingly the Academy of Finland and the Foundation of Emil Aaltonen.

References

[1] T. Stevens, E. Creigton, A. Gordon, M. MacNicol, J. Chem. Soc. (1928) 3193–3197.
[2] T. Stevens, J. Chem. Soc. (1930) 2107–2119.
[3] T. Stevens, W. Snedden, E. Stiller, T. Thomson, J. Chem. Soc. (1930) 2119–2125.
[4] T. Thomson, T. Stevens, J. Chem. Soc. (1932) 55–69.
[5] T. Thomson, T. Stevens, J. Chem. Soc. (1932) 69–73.
[6] J. Dunn, T. Stevens, J. Chem. Soc. (1932) 1926–1931.
[7] T. Thomson, T. Stevens, J. Chem. Soc. 11 (1932) 1932–1940.
[8] K. Laidler, C. Hinshelwood, J. Chem. Soc. 11 (1938) 858–862.
[9] K. Akagi, S. Oae, M. Murakami, J. Am. Chem. Soc. 79 (1957) 3118–3120.
[10] H. Sommer, H. Lipp, L. Jackson, J. Org. Chem. 36 (1971) 824–828.
[11] J. Dockx, Synthesis (1973) 441–456.
[12] S. Haas, H. Hoffmann, Prog. Polym. Sci. 101 (1996) 131–134.
[13] F. Menger, J. Keiper, Angew. Chem. Int. Ed. 39 (2000) 1907–1920.
[14] M. In, V. Bec, O. Aguerre-Chariol, R. Zana, Langmuir 16 (2000) 141–148.
[15] B. Bales, R. Zana, J. Phys. Chem. B 106 (2002) 1926–1939.
[16] A. Wiacek, E. Chibowski, K. Wilk, Colloids Surf. A 193 (2001) 51–60.
[17] X. Li, S. Goh, Y. Lai, S.-M. Deng, J. Appl. Polym. Sci. 73 (1999) 2771–2777.
[18] T. Ooi, Y. Uematsu, M. Kameda, K. Maruoka, Angew. Chem. Int. Ed. 41 (2002) 1551–1554.
[19] J. Shimizu, T. Nogami, H. Mikawa, Solid Sate Ionics 14 (1984) 153–157.
[20] K. Cathro, K. Cedzynska, D. Constable, P. Hoobin, J. Power Sources 18 (4) (1986) 349–370.
[21] P. Hoobin, K. Cathro, J. Niere, J. Appl. Electroehem. 19 (6) (1989) 943–945.
[22] K. Cedzynska, Electrochim. Acta 40 (8) (1995) 971–976.
[23] K. Murayama, K. Aoki, Chem. Commun. 5 (1998) 607–608.
[24] C. Schalley, T. Martin, U. Obst, J. Rebek, J. Am. Chem. Soc. 121 (1999) 2133–2138.
[25] A. Shivanyuk, J. Rebek, Chem. Commun. 22 (2001) 2374–2375.
[26] H. Mansikkamäki, M. Nissinen, K. Rissanen, Chem. Commun. 17 (2002) 1902–1903.
[27] H. Mansikkamäki, M. Nissinen, C. Schalley, K. Rissanen, New. J. Chem. 27 (2003) 88–97.
[28] B. Lowe, H. Rendall, Trans. Faraday Soc. 67 (8) (1971) 2318–2327.
[29] B. Lowe, H. Rendall, J. Chem. Soc., Faraday Trans. 1: Phys. Chem. Condens. Phases 68 (12) (1972) 2191–2202.
[30] Y. Kiso, T. Hirokawa, Chem. Lett. (8) (1979) 891–894.
[31] L. Blanco, A. Gomez, G. Bermudez, Acta Sud Am. Quim. 1 (2) (1981) 107–118.
[32] L. Blanco, A. Oviedo, Acta Sud Am. Quim. 3 (2) (1983) 57–65.
[33] L. Blanco, A. Oviedo, N. Vargas, Acta Sud Am. Quim. 3 (1) (1983) 29–35.
[34] J. Barthel, R. Wachter, G. Schmeer, H. Hilbinger, J. Solution Chem. 15 (7) (1986) 531–550.
[35] M. Ue, Electrochim. Acta 39 (13) (1994) 2083–2087.
[36] A. Abbott, T. Claxton, J. Fawcett, J. Harper, J. Chem. Soc. Faraday Trans. 92 (10) (1996) 1747–1749.
[37] A. Abbott, D. Schiffrin, J. Chem. Soc. Faraday Trans. 86 (9) (1990) 1453–1459.
[38] A. Abbott, G. Griffith, J. Harper, J. Chem. Soc. Faraday Trans. 93 (4) (1997) 577–582.
[39] P. Gassman, D. Heckert, J. Organic Chem. 30 (8) (1965) 2859–2861.
[40] E. Randall, D. Shaw, Spectrochim. Acta, Part A: Molec. Biomolec. Spectrosc. 23 (5) (1967) 1235–1242.
[41] K. Tori, T. Iwata, K. Aono, M. Otsuru, T. Nakagawa, Chem. Pharmaceut. Bull. 15 (3) (1967) 329–336.
[42] B. Schueler, F. Krueger, Organic Mass Spectrometry 14 (8) (1979) 439–441.
[43] J. Ropponen, M. Lahtinen, S. Busi, M. Nissinen, E. Kolehmainen, K. Rissanen, New J. Chem. 28 (12) (2004) 1426–1430.
[44] S. Busi, M. Lahtinen, J. Ropponen, J. Valkonen, K. Rissanen, J. Solid State Chem. 177 (2004) 3757–3767.
[45] P. Wasserscheid, W. Keim, Angew. Chem. Int. Ed. 39 (2000) 3772–3789 (and references therein).
[46] D. Zhao, M. Wu, Y. Kou, E. Min, Cataly. Today 74 (2002) 157–189.
[47] E. Hassoun, M. Abraham, V. Kini, M. Al-Ghafri, A. Abushaban, Res. Commun. Pharmacol. Toxicol. 7 (2002) 23–31.
[48] J. Dupont, R. de Souza, P. Suarez, Chem. Rev. 102 (2002) 3667–3692.
[49] S. Sugden, H. Wilkins, J. Chem. Soc. (1929) 1291–1298 (and references therein).
[50] C. Swain, A. Ohno, D. Roe, R. Brown, T. Maugh II, J. Am. Chem. Soc. 89 (1967) 2648–2649.
[51] S. Nemeth, A. Robinson, N. Campbell, Abstracts of Papers, 226th ACS National Meeting, New York, NY, United States, Septemper 7–11, 2003.
[52] M. Uzagare, Y. Sanghvi, M. Salunkhe, Green Chem. 5 (2003) 370–372.
[53] E. Hassoun, M. Abraham, V. Kini, M. Al-Ghafri, A. Abushaban, Res. Commun. Pharmacol. Toxicol. 7 (2002) 23–31.
[54] E. Turner, C. Pye, R. Singer, J. Phys. Chem. A 107 (2003) 2277–2288.
[55] A. Riisager, R. Fehrmann, R. van Hal, P. Wasserscheid, Abstracts of Papers, 226th ACS National Meeting, New York, NY, United States, September 7–11, 2003, IEC-042.

[56] J. Revell, A. Ganesan, Org. Lett. 4 (2002) 3071–3073.
[57] R. Brown, P. Dyson, D. Ellis, T. Welton, Chem. Commun. 18 (2001) 1862–1863.
[58] J. Boon, J. Levisky, J. Pflug, J. Wilkes, J. Org. Chem. 51 (1986) 480–483.
[59] K. Seddon, C. Hardacre, B. Mcauley, Patent, PCT International Applications, 2003.
[60] J. Ross, J. Xiao, Green Chem. 4 (2002) 129–133.
[61] S. Nara, J. Harjani, M. Salunkhe, J. Org. Chem. 66 (2001) 8616–8620.
[62] T. Sutto, P. Trulove, H. De Long, Proceedings—Electrochemical Society 19 (2002) 54–62.
[63] C. Brazel, M. Benton, Abstracts of Papers, 224th ACS National Meeting, Boston, MA, United States, August 18–22, 2002.
[64] M. Benton, C. Brazel, Polymer Preprints (American Chemical Society, Division of Polymer Chemistry) 43 (2002) 881–882.
[65] S. Fry, N. Pienta, J. Am. Chem. Soc. 107 (1985) 6399–6400.
[66] Y. Chauvin, B. Gilbert, I. Guibard, J. Chem. Soc. Chem. Commun. 11 (1990) 1715–1716.
[67] R.T. Carlin, J. Wilkes, J. Mol. Catal. 63 (1990) 125–129.
[68] J. Wilkes, M. Zaworotko, J. Chem. Soc. Chem. Commun. (1992) 965–967.
[69] Y. Chauvin, L. Muβmann, H. Olivier, Angew. Chem. Int. Ed. Engl. 34 (1996) 2698–2700.
[70] A.J.M. Duisenberg, L.M.J. Kroon-Batenburg, A.M.M. Schreurs, J. Appl. Cryst. (2003) 220–229.
[71] A. Altomare, G. Cascarano, C. Giacovazzo, A. Guagliardi, SIR92: a program for crystal structure solution, J. Appl. Crystallogr. 26 (1993) 343–350.
[72] A. Altomare, M. Burla, M. Camalli, G. Cascarano, C. Giacovazzo, A. Guagliardi, A. Moliterni, G. Polidori, R. Spagna, SIR97: a program for crystal structure solution, J. Appl. Cryst. 32 (1999) 115–119.
[73] M.C. Burla, M. Camalli, B. Carrozzini, G.L. Cascarano, C. Giacovazzo, G. Polidori, R. Spagna, SIR2002: a new direct methods program for automatic solution and refinement of crystal structures, J. Appl. Cryst. 36 (2003) 1103.
[74] G.M. Sheldrick, SHELXS-97: a program for crystal structure analysis, Acta Crystallogr. A 46 (1990) 467–473.
[75] G.M. Sheldrick, SHELXL-97: A Program for Crystal Structure Refinement, University of Gottingen, Germany, 1997.
[76] K. Branderburg, DIAMOND, v 3.0b, Crystal Impact GbR Bonn, Germany, 2005.
[77] J. Gordon, J. Am. Chem. Soc. 87 (19) (1965) 4347–4358.
[78] T. Coker, J. Ambrose, G. Janz, J. Am. Chem. Soc. 92 (18) (1970) 5293–5297.
[79] H. House, E. Feng, N. Peet, J. Org. Chem. 36 (16) (1971) 2371–2375.
[80] M. Godlewska, S. Wrobel, B. Borzecka-Prokop, M. Michalec, P. Dynarowicz, Mol. Cryst. Liq. Cryst. 300 (1997) 113–126.
[81] E. Alami, H. Levy, R. Zana, P. Weber, A. Skoulos, Liquid Crystals 13 (1993) 201–212.
[82] H. Mansikkamäki, M. Nissinen, K. Rissanen, Angew. Chem. Int. Ed. 43 (2004) 1243–1246.